Systematic study of the structural parameters affecting the self-assembly of cyclic peptide–poly(ethylene glycol) conjugates

Edward. D. H. Mansfield, Matthias Hartlieb, Sylvain Catrouillet, Julia Y. Rho, Sophie C. Larnaudie, Sarah. E. Rogers, Joaquin Sanchis, Johannes C. Brendel, and Sébastien Perrier

Published version information:

Citation: EDH Mansfield et al. "Systematic study of the structural parameters affecting the self-assembly of cyclic peptide–poly(ethylene glycol) conjugates." Soft Matter, vol. 14, no. 30 (2018): 6320-6326.

DOI: 10.1039/C8SM01133H

Journal Name

ARTICLE

Systematic study of the structural parameters affecting the self-assembly of cyclic peptide-poly(ethylene glycol) conjugates

Received 00th January 20xx,
Accepted 00th January 20xx

DOI: 10.1039/x0xx00000x

www.rsc.org/

Edward. D. H. Mansfield,[a, ‡] Matthias Hartlieb,[a, ‡] Sylvain Catrouillet,[a, †] Julia Y. Rho,[a] Sophie C. Larnaudie,[a] Sarah. E. Rogers,[b] Joaquin Sanchis,[c] Johannes C. Brendel,[a, ‖] Sébastien Perrier[a, c, d,*]

Self-assembling cyclic peptides (CP) consisting of amino acids with alternating D- and L- chirality form nanotubes by hydrogen bonding, hydrophobic interactions, and π-π stacking in solution. These highly dynamic materials are emerging as promising supramolecular systems for a wide range of biomedical applications. Herein, we discuss how varying the polymer conformation (linear vs brush), as well as the number of polymer arms per peptide unimer affects the self-assembly of PEGylated cyclic peptides in different solvents, using Small Angle Neutron Scattering. Using the derived information, strong correlations were drawn between the size of the aggregates, solvent polarity, and its ability to compete for hydrogen bonding interactions between the peptide unimers. Using these data, it could be possible to engineer cyclic peptide nanotubes of a controlled length.

Introduction

Self-assembling cyclic peptides (CPs) consisting of an even number of amino acids with alternating chirality, were first introduced by Ghadiri in the 1990's. By taking advantage of antiparallel β-sheet formation, the peptide subunits are able to interact and form supramolecular nanotubes.[1, 2] The alternating D- and L- chirality of the involved amino acids, permits the peptide to adopt a flat disk-like conformation; permitting them to stack neatly on top of each other, [3, 4] and self-assemble through electrostatic/hydrophobic interactions, π-π-stacking, and hydrogen bonding.

A major drawback of these materials is their tendency to form lateral aggregates which drastically reduces their solubility in many solvents, and thus reduces the number of potential applications.[5] One solution is to conjugate polymers to the periphery of the peptide monomer,[6] allowing them to act as a shield against the formation lateral aggregates. In addition, this strategy greatly improves the solubility of the peptide unimers; making them suitable for a wide range in biomedical applications. These CP-polymer conjugates, as well as their unconjugated equivalents, have be utilized for multiple applications including antimicrobial materials,[7, 8] the formation of trans-membrane channels[9-11] and molecular electronics.[12] Recently, research has focused on their application in a biomedical context, particular as drug delivery vectors and bio-imaging tools.[13, 14]

Although a large volume of research has been carried out on the applications of CP-polymer nanotubes, less work has been carried out looking at the fundamental properties of the self-assembly process. By designing CPs with reactive side chains, it is possible to diversify the self-assembly process by changing the polymer corona, which can lead to different properties. Indeed, Couet and Biesalski, however, have shown that both the size of the polymer and grafting density can affect the overall length of the tube.[15] Further simulation studied carried out by Benjamin and Keten, who looked specifically on the association of CPs with a different number of conjugated polymers on the self-assembly, revealed drastically different free energy profiles, depending on the number of conjugated polymer arms, where an additional arm incurs an entropic penalty which reduces self-assembly in a non-linear fashion.[16, 17]

Previously, CPs conjugated with polymers, such as poly(2-oxazoline)s,[18] N-acryloylmorpholine,[19] poly(2-(diisopropylamino)ethyl methacrylate),[20] poly(dimethylamino ethyl methacrylate),[21] or hydroxyethylacrylamide[13, 22] have been studied in this regard, however to date most of the research has focused on the use of poly(ethylene glycol) (PEG).[23-26] Given this, the present study looks to further our understanding of CP conjugates, by looking at both the

[a] Department of Chemistry, University of Warwick, Gibbet Hill Road, Coventry CV4 7AL, United Kingdom;
[b] ISIS Spallation Neutron Source, Science and Technology Facilities Council, Rutherford Appleton Laboratory, Harwell Science and Innovation Campus, Didcot, OX11 0QX, UK
[c] Faculty of Pharmacy and Pharmaceutical Sciences, Monash University, 381 Royal Parade, Parkville, VIC 3052, Australia.
[d] Warwick Medical School, The University of Warwick, Coventry CV4 7AL, U.K.;

† Current address: Institut Charles Gerhardt Montpellier UMR5253 CNRS-UM-ENSCM, Université de Montpellier F-34095 Montpellier, France
‖ Current address: Jena Center for Soft Matter (JCSM), Friedrich-Schiller-University, Philosophenweg 7, 7743 Jena, Germany.
‡ Authors contributed equally to the manuscript

grafting density and polymer architecture on the self-assembly process, as well as how the choice of solvent can affect the ultimate length of the nanotube. PEG was chosen in these studies, due to its wide use in biological applications, easy manipulation of the architecture (commercially available linear PEG, or a synthetic polyPEG acrylate brush), and solubility in a wide range of solvents. The influence of steric repulsion by the polymers on the hydrogen bond mediated stacking process, investigated using Small Angle Neutron Scattering (SANS), and was found to be a key factor in determining the length of the resulting structures. Following on, the number of polymer arms per peptide subunit was studied in various solvents in order to probe the influence of polarity and hydrogen bond capacity on the formation of nanotubes, providing insights into routes by which the assembly process can be controlled.

Results and discussion

Herein the influence of different PEG-based polymers on the self-assembly of unimeric CP's into nanotubes is described. Two different parameters were considered: 1) the architecture of the polymer chain (linear *vs* brush), allowing us to vary the steric hindrance around the CP core, and 2) the number of polymer chains per CP, its influence on self-assembly, and the effects of different solvents on tubular length. For the first approach, CPs were decorated with either linear PEG (PEG) or a PEG-bottle brush copolymer (PPEGA), whilst the second used only linear PEG.

Cyclic peptide synthesis

CPs with different compositions were synthesised using solid-phase peptide synthesis according to previously used methods.[19] In order to investigate the influence of number of polymer arms on self-assembly, CPs with a varying number of Lysine residues (Lys, used as attachment points) were synthesised. As an alternating chirality is required to form nanotubes, Leucine (Leu) was chosen as a D-amino acid and was positioned between each Lys/Tryptophan (Trp) subunit. For CPs with a decreased number of arms, Lys residues are replaced with Trp, in order to aid the self-assembly process by hydrophobic interactions and π-π- stacking. The overall structure can be described as cyclo(L -Trp- D -Leu- L -X- D -Leu- L -X- D -Leu- L -X- D -Leu), where X is either Trp or Lys. In the case of the 2-arm peptide, Lys residues were introduced on opposite sides of the cycle (Figure 1).

The linear precursors were synthesised using a trityl resin, allowing the peptide to be synthesised and cleaved without removal of the Boc-protecting groups. Cyclization was performed under dilute conditions in the presence of 4-(4,6-dimethoxy-1,3,5-triazin-2-yl)-4-methylmorpholinium tetrafluoroborate (DMTMM·BF_4) as a coupling agent. This reagent does not require any additional base, allowing for the reaction to be performed over multiple days without the risk of isomerising the amino acids. After the cyclic peptide was purified, the Boc-groups were removed using trifluoro acetic acid (TFA) to yield the final peptide (structures **3**, **6** and **9**, for one-, two-, and three-armed-peptides, respectively, Figure 1).

All intermediate, as well as final products, were characterized by ESI-mass spectrometry (Figure S1 - S9) and NMR spectroscopy (Figures S10 - S12) to prove identity and purity. ESI measurements of the linear peptides following synthesis/cleavage show m/z values corresponding to the desired product, in which the C-terminal acid group was transformed into either a potassium or sodium salt.

After cyclization, these species cannot be observed and were

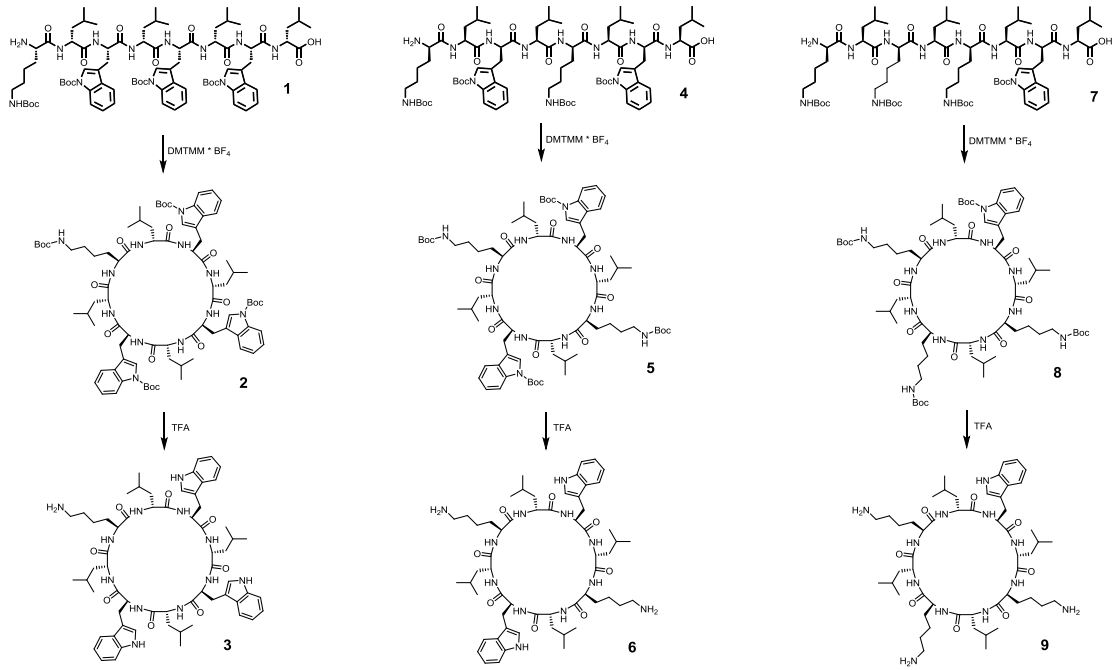

Figure 1: Schematic representation showing the synthesis of cyclic peptides with varying numbers of lysine moieties.

replaced with peaks associated with the cyclized product. Subsequent deprotection resulted in a shift to lower m/z values. ^{1}H-NMR spectroscopy further confirmed identify and purity of the cyclic peptides, as well as the quantitative deprotection. The cyclization was monitored by analysing a shift in the peak associated with the N-terminal CH-group in the peptide backbone (δ = 4.2).

Conjugate synthesis

Two different polymer architectures were utilised in this study. While the linear PEG-NHS (MW=2 kDa) was commercially available, the bottle-brush PEGA (DP 10) was synthesised *via* RAFT polymerization, in order to yield a dense bottle brush PPEGA.

As such, the brush copolymer was synthesised using an *N*-hydroxy succinimide (NHS) functionalised chain transfer agent (CTA), allowing the resulting polymer to be grafted to Lys residues on the cyclic peptide. This strategy has previously been employed to generate CP-polymer conjugates, using RAFT polymerization.[9, 11, 19] Conversion of the monomer to polymer was monitored by ^{1}H-NMR spectroscopy (Figure S13) and the size distribution was determined using size exclusion chromatography (SEC) (Figure S14). The resulting polymer showed a monomodal size distribution and a narrow dispersity (Table S2).

For conjugation, both polymer types were covalently linked to the CP *via* amidation onto the Lys moieties, using an NHS-activated carboxylic acid ω-chain end. Due to the strong aggregation tendency of the unconjugated cyclic peptide, the reaction took place in DMF, as it is expected to disrupt hydrogen bonds by competitive interaction.[27] The coupling reaction was monitored by SEC, and the product exhibited an increased molecular weight compared to the CP unimer. After completion (3 days, Figure S15) the mixture was purified by centrifugation-assisted dialysis (10 kDa MWCO) to remove any excess polymer and reagents. As the CP-polymer conjugates form nanotubes in water, the molecular weight is large enough to be above the MWCO of the dialysis tube, allowing for effective removal of the polymer and not the conjugate.

The final compounds, summarised in Figure 2, were then lyophilised and re-analysed by SEC. They exhibited monomodal size distributions with low dispersities (Đ = 1.12, Figure S16). In all cases, the polymer (linear or brush) was added in excess to ensure all Lys moieties had reacted.

Structural characterisation using SANS

SANS is a powerful tool in the field of supramolecular chemistry as it allows for structural assessment of a self-assembled system in response to different environmental and external stimuli, such as temperature, pH, or solvent. Additionally, by modelling the data to different form factors, it is possible to critically assess the structure, dimensions, and number of aggregation (N_{agg}) for self-assembled species. In the present study, SANS was used to study the structural parameters, including size and morphology, of the different CP-polymer conjugates in a range of different solvents.

Following data collection, the scattering profile for each sample was corrected for transmission and background scattering from the respective solvent before being plotted on an absolute scale as a one-dimensional scattering cross-section. The scattering cross-section was measured over a Q-range of 0.004 - 0.7 Å^{-1} (SANS2D), or 0.006 – 0.24 Å^{-1} (D11). In some cases, longer Q-ranges were exploited to gain further information at the lowest Q-values, where no turn-over was reached The data was then modelled using a variety of different form factors, however the most reliable fits could be obtained with either a Gaussian coil, comb, or cylindrical micelle (described herein as a hairy cylinder). For non-assembled systems with a conjugated linear PEG, the best fits were obtained with a Gaussian coil model, while a comb model accurate described the data obtained for conjugates with a PEGA brush.

For self-assembled species, a cylindrical micelle with attached polymer chains ("CYL+CHAINS(RW)")[28] or hairy cylinder model was used, as fitting to a cylinder or core-shell cylinder yielded unrealistic parameter values. Further details on the SANS experimental set-up, data analysis and fitting parameters can be found in the Supplementary Information, S17, 18, and 19. A reliable fit was considered when the Chi^{2} values were <5. In some cases higher Chi^{2} values were obtained due to high incoherent scattering in the sample (e.g. 2-arm CP-PEG in DMSO. In all cases, the SLD values were calculated and used as fixed parameters. Additionally, the radius of the core was fixed at 5 Å, which represents that of the cyclic peptide itself.[3]

Linear vs. brush polymer

Firstly, the effect of PEG architecture (linear *vs* brush) was studied. It was hypothesised that, due to the more sterically demanding brush-conformation, self-assembly would be reduced or completely inhibited for these systems, as predicted by the previously described simulation studies. The two-armed brush conjugate was compared with a two-armed linear PEG-CP conjugate in D_2O (Compounds **14** (MW=5080) and **11** (MW=11080), respectively).

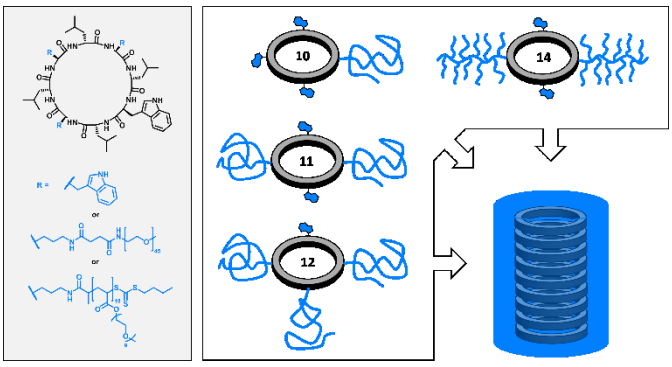

Figure 2: Summary of the different CP-polymer conjugates used in this study

Compound **14**, having two PPEGA arms each with a DP of 10, was the most sterically challenged conjugate used in this study, and little self-assembly was observed. Indeed, the best model for this system was to a comb, providing a reliable fit over the whole Q-range (Figure 3). By determining the molecular weight of this system (see SI for details), a N_{agg} of 3 was calculated (molecular weight determined by SANS divided by the molecular weight of the unimer). Given the steric hindrance caused by grafting a dense brush polymer to a single cyclic peptide, it is highly plausible that this system assembles in very small aggregates, or not at all. Comparing this to the linear counterpart, fitting the conjugate to a comb model yielded poor fits and so data were modelled more reliably to a hairy cylinder model, resulting in a N_{agg} of 22 (Chi^2 4.5).

The results of this study clearly show that steric hindrance around the peptide core plays an important role in determine the structure of the resulting nanotube.

Effect of solvent and number of polymer arms on self-assembly

Further to looking at polymer architecture, the effect of number of arms vs solvent was also probed. Here, CPs were synthesised with a different number of conjugated linear polymer chains. These compounds were dissolved in a variety of deuterated solvents, with the aim to assess how the degree of hydrogen bond interaction and hydrophobicity influences the final assembly. Here, 1-arm, 2-arm, and 3-arm conjugated cyclic peptides (Compounds **10**, **11**, and **12**, respectively) were dissolved in either deuterated N,N-Dimethylformaldehyde (d-DMF), deuterated dimethyl sulfoxide (d-DMSO), deuterated dichloromethane (d-DCM), deuterated tetrahydrofuran (d-THF), deuterated toluene (d-Toluene) or D_2O at a concentration of 5 mg mL^{-1}.

The one-armed peptide (**10**) could not be dissolved in toluene, and was not measured as a result. Again, the data was modelled using SASfit,[28] and is summarised in Figure 4.

It should be noted that for some samples (for example 1-arm CP in DMSO), an upturn at low Q was observed, suggesting the formation of larger aggregates. To incorporate this into the model, an extended Guinier form factor was considered as an additive to the model, improving the reliability of the fit (see SI for details).

As previously discussed, the best fits for the self-assembled species used the hairy-cylinder model, in D_2O, d-toluene, d-DCM and d-THF. A Q^{-1} dependency, which is characteristic of cylindrical structure, was found for all the studied systems in these solvents. Additionally, by looking at the turn-over in the Guinier region (low Q range), the length of the cylinder could be precisely determined. In some cases (such as the 1-arm CP in D_2O), no turn-over was observed, and the scattering continued at a Q^{-1} dependency. For these data sets, a finite value for tube length could not be obtained, as it exceeds the window of observation for SANS. For analysis purposes it was set at 2000 Å (the absolute limit of detection using the se-up employed) as a result, which corresponds to a N_{agg} >400. To critically compare the effect of number of arms and solvent, the values for N_{agg} were determined for all systems, summarised in Figure 5.

Looking at these data, it is clear that the number of aggregation is highly dependent on both solvent and the number of polymer arms attached to the peptide unimer. It is likely that by increasing the number of polymer chains grafted onto the peptide molecule, or replacing the polymer with a sterically more demanding macromolecule, the degree of aggregation decreases significantly. This is also confirmed in the present study, where a PEG brush was found to drastically reduce the N_{agg}. If this is taken into consideration when interpreting the data in Figure 5, the increased number of polymer chains per peptide clearly provides enough steric hindrance to drastically reduce the aggregation for the majority of the solvent systems studied.

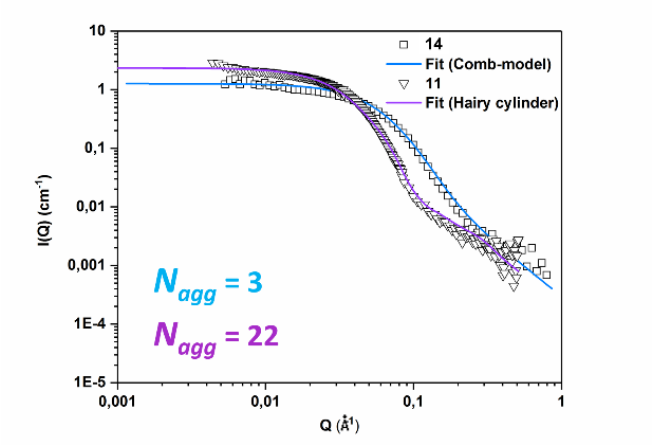

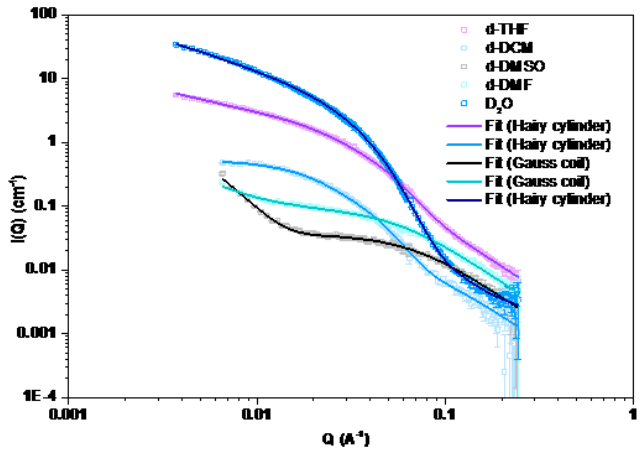

Figure 3: SANS data and fits of A) conjugate **14** ($CP(PPEGA_{10})_2$, 10 mg mL^{-1}) in D_2O and B) conjugate **11** ($CP(PEG)_2$, 10 mg mL^{-1}) in D_2O.

Figure 4: Scattering profiles for compound 10 in various solvents and their respective fits. Details on the models used and parameters can be found in Figures S17 – S19, Tables S4 – S6, including the fits for 2- and 3-arm cyclic peptides

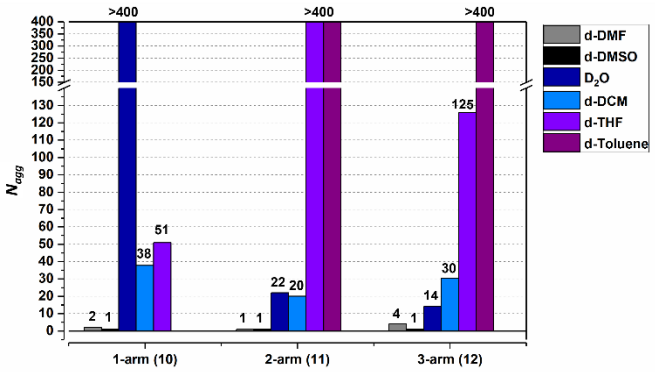

Figure 5: N_{agg} for CP-polymer conjugates with either one, two, or three polymer arms per peptide in different solvents.

This effect is most noticeable in D_2O, where the N_{agg} is reduced form >300 (1-arm) to 22 (2-arm), and 14 (3-arm). A similar trend is seen in DCM (N_{agg} 38 to 30). In toluene, both the 2- and 3-arm peptides show the formation of long cylindrical structures. In both these cases, the final length of the tube could not be determined as it was outside the window of observation for the SANS set-up employed, and is presented as >300 as a result (similar to the 1-arm peptide in D_2O). Toluene has the lowest hydrogen bond capability amongst the solvents investigated in this study, and so the peptide has little competition resulting in the formation of long tubes. The poor solubility of the 1-arm peptide in toluene further supports this hypothesis.

In DMF and DMSO, the data was best represented by a fit using a Gaussian chain form factor, and no Q^{-1} was be observed, suggesting the presence of unimeric species. The upturn of the scattering data at low Q-values indicates the presence of larger aggregates, and was thus fitted to an extended Guinier form factor. This form factor provided information on the Rg of the aggregate, and also the structure. The best fit was obtained when the α value was fixed at 2 (representing non-defined lamellar aggregates).[29] Fixing α at 0 (sphere) or 1 (cylinder) resulted in poor quality fits, as represented by high Chi^2 values. The N_{agg}, determined by comparison of the Mw with that of the unimer, shows that unimeric and/or small oligomeric species are present (N_{agg} <4), which is independent on the number of arms.

Interestingly, in THF the N_{agg} increases from 79 to >300 when the number of arms is increased from one to two, however decreases to 127 upon addition of another PEG chain (3-arm). This unusual behaviour can be ascribed to two compounding factors. The decrease in N_{agg} between the 2- and 3-armed conjugates is likely the result of increased steric demand on the conjugated polymer shell, as was observed in D_2O and DCM. Additionally, the polymer shell provides protection of the hydrogen bonding sites from solvent molecules as was previously reported.[27] While one polymer chain per unimer is not able to sufficiently shield the peptide from the solvent, the addition of a second provides a shell able to protect the hydrogen bonding sites, thus causing an increase in the N_{agg}. However, additional polymer chains only result in a greater steric demand around the peptide core, causing the N_{agg} to decrease again. It has been shown for helix-PEG conjugates that the polymer shell can actually stabilise the assembly, which could result in smaller tubes, although this is dependent on the penalty caused by steric hinderence[30] In the case presented here, it is possible that both phenomena are occurring; a stabilisation caused by the interacting polymer chains, whilst the steric repulsion causes a disassembly process.

It is clear from these data that upon addition of an additional polymer arm, the steric hindrance around the peptide core increases, thus causing a decrease in the N_{agg}; the exception being THF. However, it is also clear that the choice of solvent plays a drastic role in self-assembly, as clear differences can be observed between the data. Given that the key interactions between the cyclic peptide monomers are hydrogen bonding, hydrophobic, and possibly π-π stacking between tryptophan residues;[31] solvents which act as competitors to one or more of these will reduce any potential aggregation, resulting in a reduction in tube length. Vice versa, solvents which promote these interactions will result in larger tube sizes. It is also important to note that the polymers with a high degree of swelling in specific solvents will increase the steric effect, thus causing a reduction in self-assembly.

This hypothesis is confirmed in the data presented here. As already discussed, the N_{agg} in both DMF and DMSO is close to 1 (N_{agg} <2 for 1 arm and 2 arm peptides, and <4 in the 3-armed peptide), due to the solvent molecules acting as competitors to hydrogen-bonding sites which is arguably the strongest driving force for self-assembly of these species.[1] While D_2O also has a high tendency to form hydrogen bonds, its ability to dissolve the non-polar peptide is limited in comparison with DMSO and DMF, meaning the solvent cannot penetrate into the peptide core as readily. As a result, the interaction between D_2O molecules with the amide and carboxylic moieties in the CP backbone is limited, resulting in long tubular assemblies being formed.
The reverse can be said about toluene; while the solvent is able to solubilize the hydrophobic peptide and interrupt potential π-π stacking, it is not able to interfere with β-sheet formation between the CP unimers, resulting in the formation of long nanotubes. The high N_{agg} values for THF support these hypotheses as the solvent is less hydrophobic than toluene but also not as competitive towards hydrogen bonds as D_2O. As a result the only limitation to the aggregation process is solubility and steric hindrance caused by the number of arms.

To further analyse these findings and draw a correlation between solvent and N_{agg}, a series of contour plots were generated whereby the polarity and the hydrogen bond acceptor ability, ß, of each solvent was plotted as a function of

N_{agg}. This was used to assess how both parameters influence the stacking (Figure 6). The hydrogen bond acceptor strength, or ß,

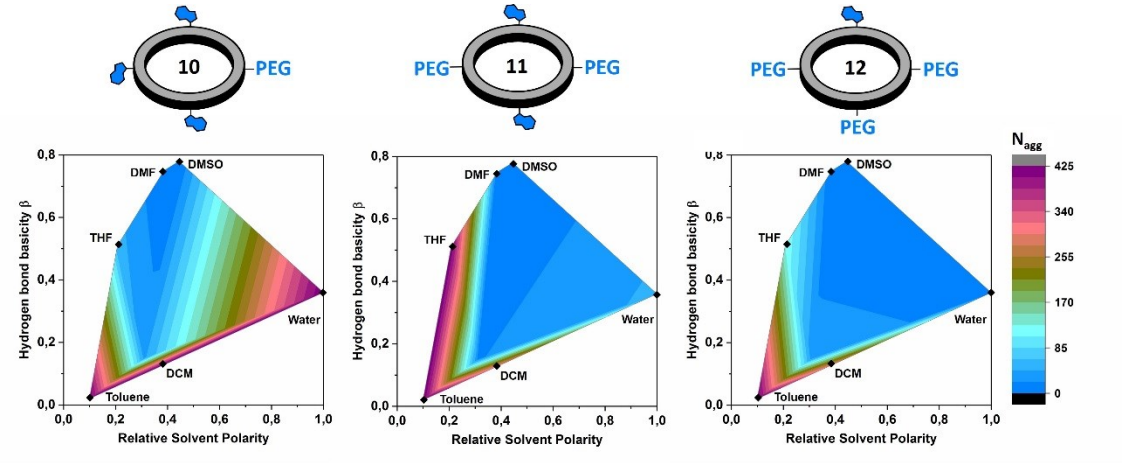

Figure 6: Contour plots of the degree of aggregation as a function of solvent polarity and the hydrogen bond acceptor capacity for one-arm (**10**), two-arm (**11**), and three-arm (**12**) cyclic peptide polymer conjugates.

can be used to describe the strength of the solvent to accept a hydrogen bond, and is based on the hydrogen bond basicity scale (pK_{HB}) of each solvent.

Compared to hydrogen bond donors, hydrogen bond acceptors can be used to describe the geometrical and chemical behaviour around the hydrogen bond site.[32] As such, solvent ß values were chosen, as they best represent the ability of the molecules to accept a hydrogen bond and reduce self-assembly. The values used were obtained from the literature.[33, 34]

Looking at the contour plots, it is clear that if both polarity and ß are low, long tubes are formed. However, in a non-polar solvent with a good hydrogen bond capacity, hydrophobic interactions are broken, resulting in smaller tubes (THF). Furthermore, if the value for ß is high and the solvent possesses a moderate polarity, as in the case of DMF and DMSO, mainly unimers are observed independently of the number of polymer
arms. An interesting effect is observed for solvents with high polarity and high hydrogen bond ability, as in the case of water.

Here the number of polymer chains, is of paramount importance. For these systems, it is possible that changing the number of tryptophan residues in the cyclic-peptide backbone (and with this the number of π-π interactions), is having an effect on self-assembly. In the case of compound **10** (CP-1 arm)**,** with three tryptophan residues and only one polymer chain, long nanotubes are formed in water. However, when the number of PEG chains increases, and number of tryptophan residues decreases, the N_{agg} is drastically decreased. This can be attributed to the increased hydrophilic nature of the conjugates. Increasing the hydrophilicity of the corona surrounding the peptide, means more water can penetrate through to the CP core, thus allowing for the water molecules to act as competitors to the hydrogen bonding sites.

Although this effect was unsurprising, the degree at which it affects the N_{agg} between the 1- and 2-arm peptide is remarkable, as a very sharp transition between long nanotubes and short tubular assemblies can be achieved with the addition of a single PEG chain. As a result, it could be that by changing the length of the PEG chain, it may be possible to tailor nanotubes with a specific N_{agg} as a function of PEG DP/number of arms; a prospect very exciting for potential drug delivery applications.

Conclusion

This study looks at how changes in structure and environment can result in drastic changes to the self-assembly of cyclic peptide-polymer nanotubes. Initially, linear and brush-like poly(ethylene glycol) macromolecules were conjugated to the periphery of cyclic peptide nanotubes. The influence of chain architecture was studied (linear *vs* brush), and it was found that the bulky brush conformation helped inhibit the self-assembly process due to steric hindrance around the peptide core, whereas its linear counterpart formed long nanotubes in solution. Following on, the effect of number of conjugated polymer arms was studied. Various solvents were used to

probe the influence of both solvent polarity and ability to interact with hydrogen bonding sites on the number of aggregation of the resulting nanotubes. It was found that in solvents with a high hydrogen bonding acceptor quality (DMF or DMSO), conjugates will mainly form unimers or oligomers, whereas in solvents with moderate hydrogen bonding capacity, the tubular length will more strongly rely on the solvents ability to overcome any hydrophobic interactions between the residues. Here the properties of the polymer corona gain more importance, as the ratio between polymer and peptide influences the overall polarity of the assembly, and consequently the ability of solvent molecules to interact with the peptide itself. Finally, solvents that will not challenge ß-sheet formation will promote the formation of long tubular assemblies despite a high tendency of competing and overcoming the forces holding the tube together.

Previous studies looking into the effect of solvent and polymer corona on the self-assembly of cyclic peptide nanotubes revealed a link between different solvent mixtures as well as tubular length.[27] However, this systematic study provides a more in-depth analysis, and demonstrates how important the periphery is when considering the design of new assemblies, and how easily the tube length can be readily manipulated by the choice of the solvent to favour either high aspect ratio structures or unimeric species. From the data presented here, it
could be possible to synthesise a range of cyclic peptide-conjugates of a controlled length for highly bespoke, novel biomedical and drug delivery applications.

Acknowledgments

We graciously thank the Royal Society Wolfson Merit Award (WM130055; SP), the Monash-Warwick Alliance (SL; SP; EM; JR; SC; JS) European Research Council (TUSUPO 647106; SP) for financial support. MH gratefully acknowledges the German Research Foundation (DFG, GZ: HA 7725/1-1) for funding. JB thanks the German Science Foundation (DFG) for granting a full postdoctoral fellowship (BR 4905/1-1) and a return grant (BR 4905/2-1). We also acknowledge the STFC for the allocation of beam time and consumables grants at ISIS (RB1510236) and ILL (Experiment 9-13-668).[35] The authors Ralf Schweins (ILL, Grenoble, France), as well as Pratik Gurnani, Tammie Barlow and Andrew Kerr for assistance with SANS.

Conflicts of interest

The authors declare no conflict of interest.

References

1. M. R. Ghadiri, J. R. Granja, R. A. Milligan, D. E. McRee and N. Khazanovich, *Nature*, 1993, **366**, 324-327.
2. N. Rodriguez-Vazquez, M. Amorin and J. R. Granja, *Organic & Biomolecular Chemistry*, 2017, **15**, 4490-4505.
3. R. Chapman, M. Danial, M. L. Koh, K. A. Jolliffe and S. Perrier, *Chemical Society reviews*, 2012, **41**, 6023-6041.
4. M. R. Silk, J. Newman, J. C. Ratcliffe, J. F. White, T. Caradoc-Davies, J. R. Price, S. Perrier, P. E. Thompson and D. K. Chalmers, *Chemical Communications*, 2017, **53**, 6613-6616.
5. N. Khazanovich, J. R. Granja, D. E. McRee, R. A. Milligan and M. R. Ghadiri, *Journal of the American Chemical Society*, 1994, **116**, 6011-6012.
6. J. Couet, J. D. J. S. Samuel, A. Kopyshev, S. Santer and M. Biesalski, *Angewandte Chemie International Edition*, 2005, **44**, 3297-3301.
7. V. Dartois, J. Sanchez-Quesada, E. Cabezas, E. Chi, C. Dubbelde, C. Dunn, J. Granja, C. Gritzen, D. Weinberger, M. R. Ghadiri and T. R. Parr, *Antimicrobial Agents and Chemotherapy*, 2005, **49**, 3302-3310.
8. S. Fernandez-Lopez, H.-S. Kim, E. C. Choi, M. Delgado, J. R. Granja, A. Khasanov, K. Kraehenbuehl, G. Long, D. A. Weinberger, K. M. Wilcoxen and M. R. Ghadiri, *Nature*, 2001, **412**, 452-455.
9. M. Danial, C. M. N. Tran, K. A. Jolliffe and S. Perrier, *Journal of the American Chemical Society*, 2014, **136**, 8018-8026.
10. M. R. Ghadiri, J. R. Granja and L. K. Buehler, *Nature*, 1994, **369**, 301-304.
11. M. Danial, C. My-Nhi Tran, P. G. Young, S. Perrier and K. A. Jolliffe, *Nat Commun*, 2013, **4**.
12. M. Mizrahi, A. Zakrassov, J. Lerner-Yardeni and N. Ashkenasy, *Nanoscale*, 2012, **4**, 518-524.
13. B. M. Blunden , R. Chapman, M. Danial, H. Lu, K. A. Jolliffe, S. Perrier and M. H. Stenzel, *Chemistry – A European Journal*, 2014, **20**, 12745-12749.
14. S. C. Larnaudie, J. C. Brendel, I. Romero-Canelón, C. Sanchez-Cano, S. Catrouillet, J. Sanchis, J. P. C. Coverdale, J.-I. Song, A. Habtemariam, P. J. Sadler, K. A. Jolliffe and S. Perrier, *Biomacromolecules*, 2018, **19**, 239-247.
15. J. Couet and M. Biesalski, *Small*, 2008, **4**, 1008-1016.
16. A. Benjamin and S. Keten, *The Journal of Physical Chemistry B*, 2016, **120**, 3425-3433.
17. L. Ruiz and S. Keten, *Soft Matter*, 2014, **10**, 851-861.
18. R. Chapman, P. J. M. Bouten, R. Hoogenboom, K. A. Jolliffe and S. Perrier, *Chemical Communications*, 2013, **49**, 6522-6524.
19. S. C. Larnaudie, J. C. Brendel, K. A. Jolliffe and S. Perrier, *Journal of Polymer Science Part A: Polymer Chemistry*, 2016, **54**, 1003-1011.
20. S. C. Larnaudie, J. C. Brendel, K. A. Jolliffe and S. Perrier, *ACS Macro Letters*, 2017, **6**, 1347-1351.
21. S. Catrouillet, J. C. Brendel, S. Larnaudie, T. Barlow, K. A. Jolliffe and S. Perrier, *ACS Macro Letters*, 2016, **5**, 1119-1123.
22. R. Chapman, K. A. Jolliffe and S. Perrier, *Polym. Chem.*, 2011, **2**, 1956-1963.
23. R. Duncan, *Journal of Controlled Release*, 2014, **190**, 371-380.
24. K. Knop, R. Hoogenboom, D. Fischer and U. S. Schubert, *Angewandte Chemie International Edition*, 2010, **49**, 6288-6308.
25. J. Y. Rho, J. C. Brendel, L. R. MacFarlane, E. D. H. Mansfield, R. Peltier, S. Rogers, M. Hartlieb and S. Perrier, *Advanced Functional Materials*, DOI: 10.1002/adfm.201704569, 1704569-n/a.

26. F. M. Veronese and G. Pasut, *Drug discovery today*, 2005, **10**, 1451-1458.
27. R. Chapman, M. L. Koh, G. G. Warr, K. A. Jolliffe and S. Perrier, *Chemical Science*, 2013, **4**, 2581-2589.
28. https://kur.web.psi.ch/sans1/SANSSoft/sasfit.html.
29. J. Andrä, J. Howe, P. Garidel, M. Rössle, W. Richter, J. Leiva-León, I. Moriyon, R. Bartels, T. Gutsmann and K. Brandenburg, *Biochemical Journal*, 2007, **406**, 297-307.
30. D. Ma, E. P. DeBenedictis, R. Lund and S. Keten, *Nanoscale*, 2016, **8**, 19334-19342.
31. D. Mandal, R. K. Tiwari, A. Nasrolahi Shirazi, D. Oh, G. Ye, A. Banerjee, A. Yadav and K. Parang, *Soft Matter*, 2013, **9**, 9465-9475.
32. J. Schwöbel, R.-U. Ebert, R. Kühne and G. Schüürmann, *Journal of Chemical Information and Modeling*, 2009, **49**, 956-962.
33. M. H. Abraham, P. L. Grellier, D. V. Prior, J. J. Morris and P. J. Taylor, *Journal of the Chemical Society, Perkin Transactions 2*, 1990, DOI: 10.1039/P29900000521, 521-529.
34. M. H. Abraham and J. A. Platts, *The Journal of Organic Chemistry*, 2001, **66**, 3484-3491.
35. S. Perrier, S. Catrouillet, P. Gurnani, A. Kerr, J. Rho and R. Schweins, 2016, DOI:10.5291/ILL-DATA. 5299-5213-5668